

# A SCHEME FOR EVALUATING THE MEAN MERIDIONAL CIRCULATION OF THE ATMOSPHERE\*

WU GUOXIONG (GUO-XIONG WU 吴国雄)

(*Institute of Atmospheric Physics, Academia Sinica, Beijing*)

AND STEFANO TIBALDI

(*European Centre for Medium-Range Weather Forecasts, Reading, U. K.*)

Received December 25, 1986; revised August 8, 1987.

## ABSTRACT

Based on the continuity of the atmosphere, a new scheme is developed to diagnose the atmospheric mean meridional circulations. ECMWF analyses four times per day of January 1982 were retrieved to evaluate the global mean meridional circulation. Investigations and calculations show that this new scheme produced more reasonable results in comparison with the traditional scheme. The existence of the double Hadley cell in the winter hemisphere is confirmed as well.

**Key words:** mean meridional circulation, double Hadley cell.

## I. INTRODUCTION

Due to the intuitiveness in atmospheric thermal balance consideration, the first plain conceptual knowledge about the mean meridional circulation (MMC) of the atmosphere was a complete hemispheric cell with rising motion at the equator and sinking at the pole (see Ref. [1]). However, the inertial effects of large-scale motions experienced are so strong that such cell should be very unstable and eventually breaks down. Even at the very beginning of the investigations concerning MMC, it was recognized that, instead of one, there should be three cells in each hemisphere. Nevertheless, it was not until the late 1940s that the mechanism of MMC became much clearer (see Ref. [2]). As a matter of fact, MMC belongs to the category of secondary circulation. Only when geostrophic and hydrostatic balances of the atmosphere are continuously destroyed by diabatic heating or eddy transfer processes, are the MMCs generated to counteract these destructive processes so that new balances can be restored (see Ref. [3]).

MMC plays very important roles in atmospheric budgets of angular momentum and energy. The inertial torque of their horizontal branch exerted upon the atmosphere balances the generation near the surface, and the transfer in the free atmos-

---

\* This study was completed in 1984 when the first author worked at ECMWF as a visiting scientist.

phere, of angular momentum. The adiabatic heating of their vertical branch is balanced by either diabatic heating or eddy heat transfer<sup>[4]</sup>. Therefore, it is important to calculate the MMC as correctly as possible.

Traditionally, MMC is calculated under the assumption that across a latitude circle, there is no net mean mass flux above 1000 hPa. Thus the zonal mean meridional and vertical wind speeds,  $\bar{v}$  and  $\bar{\omega}$  respectively, at 1000 hPa can be regarded as zero. In other words, at lower boundary (1000 hPa), values of stream-function  $X$  of MMC may be taken as zero. To achieve these, one has to compute the vertical average of  $\bar{v}$  about 1000 hPa, then subtract it from the original  $\bar{v}$  field to construct a modified meridional wind field  $v^*$ . The  $\bar{\omega}$  field is then recomputed as  $\omega^*$  from the  $v^*$  by virtue of continuity equation. The calculation of  $X$  is now straightforward via the definition of (2.2) or (2.3) since at boundaries, values of  $X$  are all zero (see Ref. [5]).

There are some problems concerning such calculation scheme. Mathematically, there exist two boundaries in both horizontal and vertical directions. Some uncertainties thus exist because the differential equations employed for calculating stream-function  $X$  are only of the first order. Secondly, it is not necessary to require that across a latitude circle, the net mass flux above a certain pressure level due to MMC should vanish, since the mean eddy mass transfer cannot be neglected. In addition, for regions where elevations are above 1000 hPa level, meteorological quantities at 1000 hPa must be extrapolated from observations at upper layers. Hence, the zonal mean data in the lower troposphere, especially below 700 hPa, suffer from such extrapolation, and serious errors might exist. This is even severer in the zonal mean wind fields  $\bar{v}$  and  $\bar{\omega}$ . On the other hand, the upper layer data are more reliable, especially over the data-dense areas. The adjustment of observation data in both horizontal and vertical directions in the traditional scheme therefore might distort the MMC even in the upper atmosphere.

A new scheme based on continuity considerations is developed here to try to avoid some uncertainties, and to keep the original data unchanged. Having derived this scheme, comparisons between the new and the traditional one are presented.

## II. CALCULATION SCHEME

In a spherical framework with pressure as the vertical coordinate, the zonally averaged continuity equation can be written as

$$\partial(\bar{\omega} \cos \varphi) / \partial P + \partial(\bar{v} \cos \varphi) / a \partial \varphi = 0, \quad (2.1)$$

where the overbar denotes zonal mean, and the other symbols have the usual meanings. The zonal mean mass flux  $X$  can be defined by a pair of equations:

$$2\pi a^2 \bar{\omega} \cos \varphi / g = -\partial X / \partial P = -A, \quad (2.2)$$

$$2\pi a \bar{v} \cos \varphi / g = \partial X / \partial \varphi = B. \quad (2.3)$$

Since the Euler condition, i. e.  $\partial A / \partial P - \partial B / \partial \varphi = 0$ , is satisfied,  $X$  is an analytical function of  $\varphi$  and  $P$ . Its total differential can be expressed as

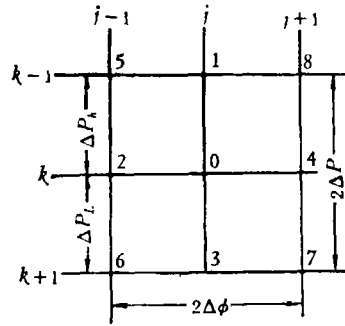


Fig. 1. The space integration scheme used to calculate the mean meridional mass flux. See text for details.

$$dX = (\partial X / \partial \varphi) d\varphi + (\partial X / \partial P) dP, \tag{2.4}$$

and any line integral of  $X$  is independent of the path. Therefore, the value of  $X$  at gridpoint 0 ( $j, k$ ) can be calculated from that at point 5 ( $j - 1, k - 1$ ) (see Fig. 1) through the following line integration

$$X_0 = X_5 + A_{15} \Delta \varphi + B_{10} \Delta P_h$$

or

$$X_0 = X_5 + A_{20} \Delta \varphi + B_{20} \Delta P_h,$$

where  $A_{jk} = (A_j + A_k) / 2$  and  $B_{jk} = (B_j + B_k) / 2$ . Upon taking the average, we then have

$$X_0 = X_5 + 0.25(A_5 + A_1 + A_2 + A_0) \Delta \varphi + 0.25(B_5 + B_1 + B_2 + B_0) P_h. \tag{2.5}$$

Using (2.5) for point 0 but from the other diagonal surrounding points, i. e. 6 ( $j - 1, k + 1$ ), 7 ( $j + 1, k + 1$ ) and 8 ( $j + 1, k - 1$ ), and taking the average, one can obtain

$$X_{j,k} = 0.25(X_{j+1,k+1} + X_{j-1,k+1} + X_{j+1,k-1} + X_{j-1,k-1}) + G_{j,k}(\bar{\omega}, \bar{v}, \varphi, P), \tag{2.6}$$

where

$$\begin{aligned} G_{j,k}(\bar{\omega}, \bar{v}, \varphi, P) = & 0.0625 \{ \Delta \varphi [(A_5 + 2A_2 + A_6) - (A_7 + 2A_4 + A_8)] \\ & - [\Delta P_L (B_6 + B_7 + B_2 + B_4 + 2B_3 + 2B_0) \\ & - \Delta P_h (B_5 + B_8 + B_2 + B_4 + 2B_1 + 2B_0)] \}. \end{aligned} \tag{2.7}$$

The boundary conditions used for the calculations are  $X = 0$  at the upper boundary ( $p = 0$ ) and at the poles (since there is no net mass flux there). At 1000 hPa,  $X$  may be obtained by using either (2.2) or (2.3). Experiments showed that the results are similar. In our calculations, (2.2) is adopted to obtain the lower boundary values, using an iteration scheme.

The method is tested in two ways. The first is to assume an ideal  $\bar{v}$  field as given by

$$\bar{v} = \bar{v}_0 \sin 6\varphi \sin (2\pi P / P_*) = -\bar{v}_0 \sin 6\theta \sin (2\pi P / P_*), \tag{2.8}$$

where  $\varphi = \theta - \pi / 2$ , and  $\bar{v}_0$  and  $P_*$  are assumed to be  $1 \text{ ms}^{-1}$  and 1050 hPa respectively. The analytical expressions for  $\bar{\omega}$  and  $X$  are then immediate:

$$\bar{\omega} = P_* \bar{v}_0 (6 \cos 6\theta + \sin 6\theta \text{ctn} \theta) [1 - \cos (2\pi P / P_*)] / 2\pi a, \tag{2.9}$$

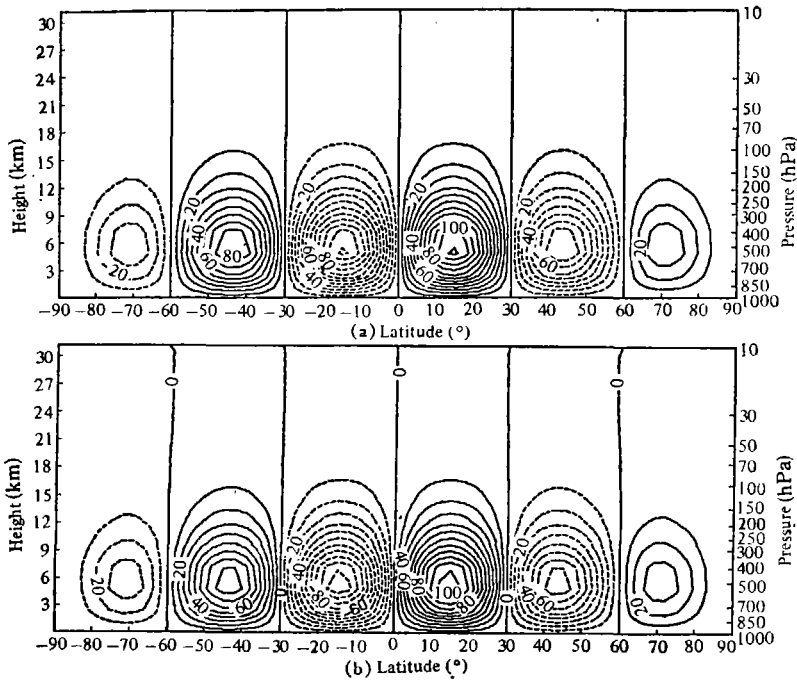


Fig. 2. The assumed analytical field of mass flux (a), and the calculated mass flux using our scheme (b). Units in  $10^6 \text{ ton} \cdot \text{s}^{-1}$ .

$$X = a\bar{v}_0 P_* \sin \theta \sin 6\theta [\cos(2\pi P/P_*) - 1]/g. \quad (2.10)$$

This analytical  $X$  field is shown in Fig. 2(a). Having these expressions for  $\bar{w}$  and  $\bar{v}$ ,  $X$  can also be obtained through (2.6), and this is shown in Fig. 2(b). The intensities of the Ferrel and Hadley cells are  $92 \times 10^6$  and  $125 \times 10^6 \text{ ton} \cdot \text{s}^{-1}$  in the calculations, and  $96 \times 10^6$  and  $131 \times 10^6 \text{ ton} \cdot \text{s}^{-1}$  in the assumed inputs, respectively. The comparison between the “true” and the “diagnosed” fields is considered satisfactory. The errors are one order of magnitude smaller than the quantities themselves, and the scheme is regarded as acceptable.

The second procedure is to recalculate the  $\bar{v}$  and  $\bar{w}$  from the diagnosed  $X$  field. They are then compared to the original  $\bar{v}$  and  $\bar{w}$  and shown respectively in Figs. 3 and 4. The flux vectors composed of  $\bar{v}$  and  $\bar{w}$  in these two different cases are also shown in Fig. 5. Our scheme reproduces the upward and poleward speeds from the equatorward and upper branches of the Hadley cells as  $2.9 \times 10^{-4} \text{ hPa} \cdot \text{s}^{-1}$  and  $0.95 \text{ m} \cdot \text{s}^{-1}$  respectively; whereas their corresponding “true” values are  $3.1 \times 10^{-4} \text{ hPa} \cdot \text{s}^{-1}$  and  $1.0 \text{ m} \cdot \text{s}^{-1}$  respectively. The general agreement is again considered satisfactory. This second procedure can be applied to the observed data and will therefore be used later to compare different methods.

### III. MEAN MERIDIONAL MASS FLUX OF THE ATMOSPHERE

#### 1. Comparisons Between the Two Schemes

In order to make comparisons between the old and new schemes, four archived

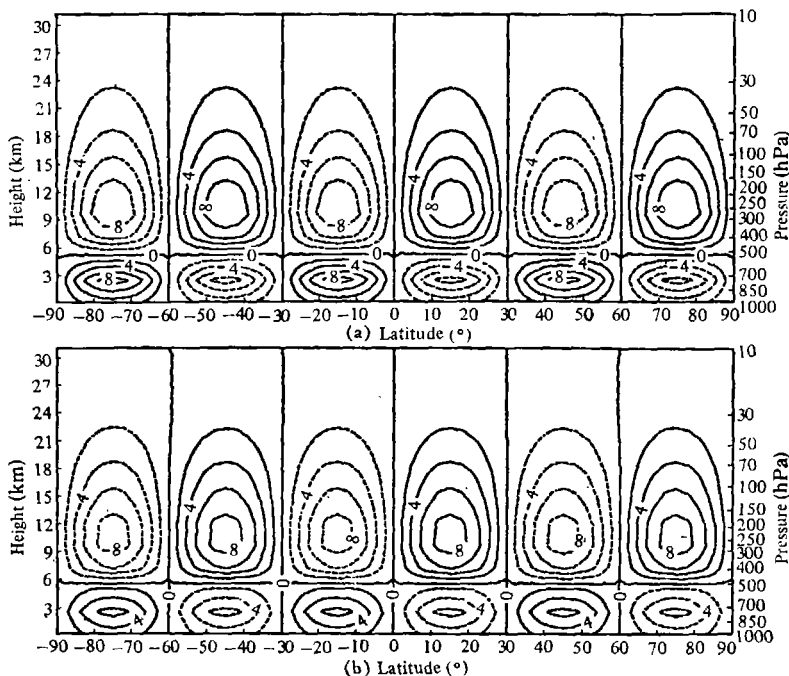


Fig. 3. The assumed analytical field of zonally averaged meridional wind  $\bar{v}$  (a), and the same field calculated using our scheme (b). Units in  $10^{-1} \text{ m} \cdot \text{s}^{-1}$ .

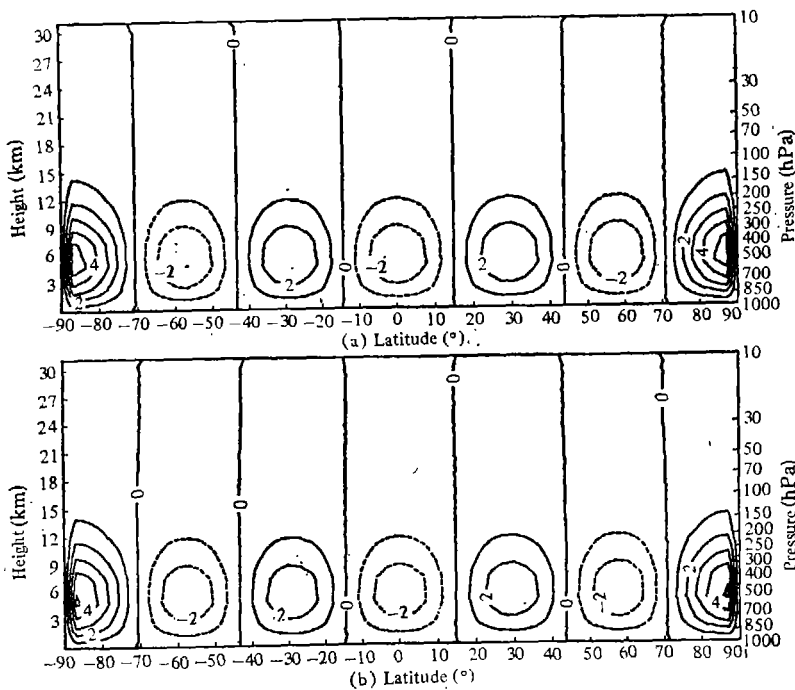


Fig. 4. The assumed analytical field of zonally averaged vertical wind  $\bar{w}$  (a), and the same field calculated using our scheme (b). Units in  $10^{-4} \text{ hPa} \cdot \text{s}^{-1}$ .

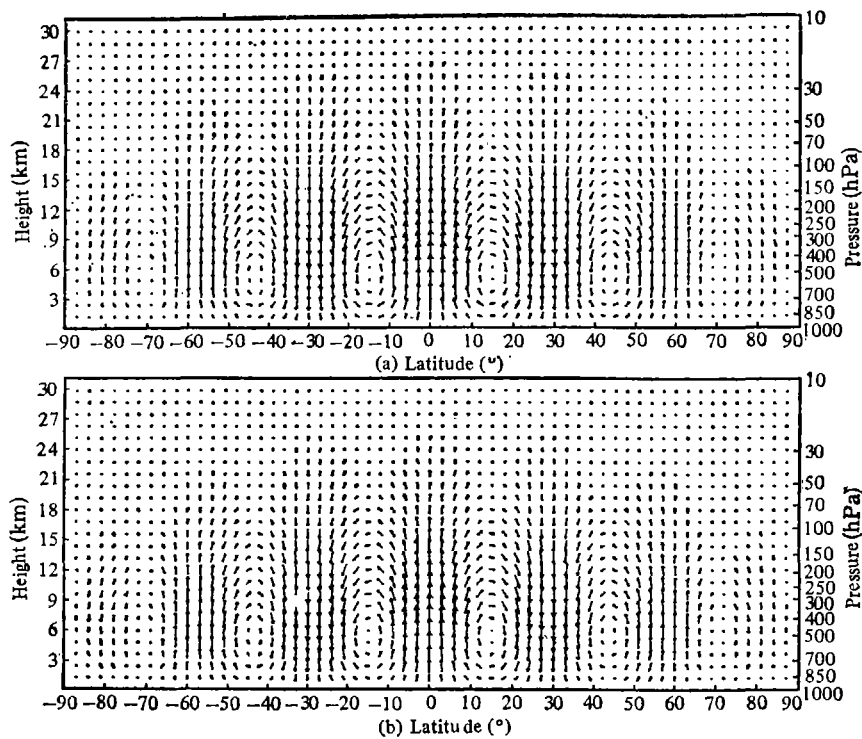


Fig. 5. The assumed analytical mass flux (a) and the recovered flux (b) derived from the calculated X field. The vertical speeds are amplified by a factor of 1000.

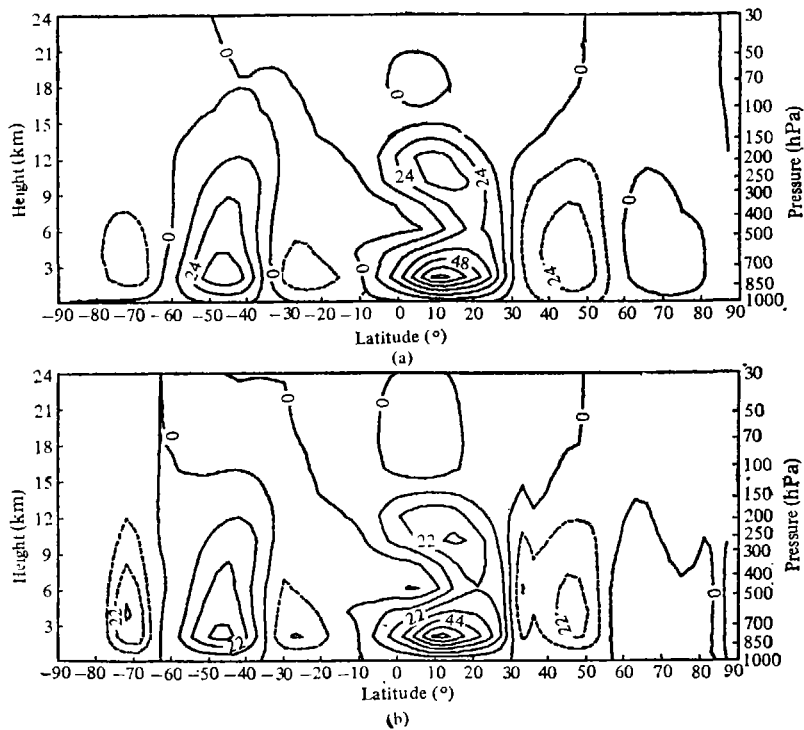


Fig. 6. The mean meridional mass flux of January 1982. Units in  $10^6 \text{ ton} \cdot \text{s}^{-1}$ .  
 (a) Computed using our scheme; (b) computed using the traditional scheme.

**Table 1**

The Intensity and Location of the Mean Meridional Circulation Centres Calculated From the Present Scheme (NEW) and From the Traditional Scheme (OLD)

		Southern Hemis.			Northern Hemis.			
NEW	X	-22	50	-27	45	86	-37	7
	Lat.	72°S	45°S	24°S	12°N	12°N	45°N	69°N
	h(hPa)	700	850	850	250	850	700	700
OLD	X	-36	39	-26	36	81	-28	10
	Lat.	72°S	45°S	27°S	12°N	12°N	48°N	63°N
	h(hPa)	700	850	850	250	850	700	700

Note: Unit:  $10^6 \text{ ton} \cdot \text{s}^{-1}$ .

**Table 2**

The Northern Hemispheric Centres of the  $\bar{v}$  Field Reproduced From the X Fields Using Our Scheme (NEW) and Using the Traditional Scheme (OLD) Compared With the Original Input Data (OBS)

	Upper Hadley Cell	Lower Hadley Cell	Ferrel Cell	Polar Cell
OBS	1.55/-0.87	1.01/-2.64	-0.48/0.57	0.26/-0.56
NEW	1.10/-0.63	0.56/-2.64	-0.41/0.57	0.20/-0.56
OLD	1.00/-0.54	0.58/-2.58	-0.36/0.64	0.21/-0.55

Note: The numbers on the left denote the speed of the upper branch, those on the right, the speed of the lower branch. Unit:  $\text{m} \cdot \text{s}^{-1}$ .

**Table 3**

The Northern Hemispheric Centres of the  $\bar{\omega}$  Field Computed From the X Fields Using Our Scheme (NEW) and the Traditional Scheme (OLD) in Comparison With the Original Input Data (OBS)

Lat.	0°N	27°N	54°N	72°N
OBS	-1.28	1.94	-1.55	0.77
NEW	-1.09	1.63	-1.39	0.60
OLD	-0.87	1.55	-1.50	0.53

Note: Units:  $10^{-4} \text{ hPa} \cdot \text{s}^{-1}$ .

data in a single day (00Z, 06Z, 12Z and 18Z) were retrieved from the ECMWF data base for January 1982. Monthly mean  $\bar{\omega}$  and  $\bar{v}$  fields were then calculated on a grid mesh in which, 13 standard pressure levels from 30 hPa to 1000 hPa in the vertical and horizontal grid lengths of 3 degrees of latitude from 87°N to 87°S were used. The mass flux calculated from these two methods are presented in Fig. 6. The intensities and locations of their centres are given in Table 1. Despite the general resemblance, our scheme gives much stronger meridional cells in mid-latitudes and tropical areas than the traditional method. Particular in the northern upper tropics, the increase of the strength of the cell due to the new scheme reaches about 25%.

Having the  $X$  field calculated, the  $\bar{v}$  and  $\bar{\omega}$  fields can be reconstructed from (2.2) and (2.3) for the sake of comparisons. The intensities of centres of  $\bar{v}$  and  $\bar{\omega}$  distributions are shown in Tables 2 and 3 respectively. Almost in all cases, the intensities and locations of different centres obtained by using the new scheme are closer to the analyses than those produced by the traditional scheme. This is more evident if the  $\bar{\omega}$  test fields are considered (see Fig. 7). All the centres reproduced from the  $X$  field in the new scheme are very well in phase with analyses. Especially, instead of one, there are two rising centres at the equator, with the lower between

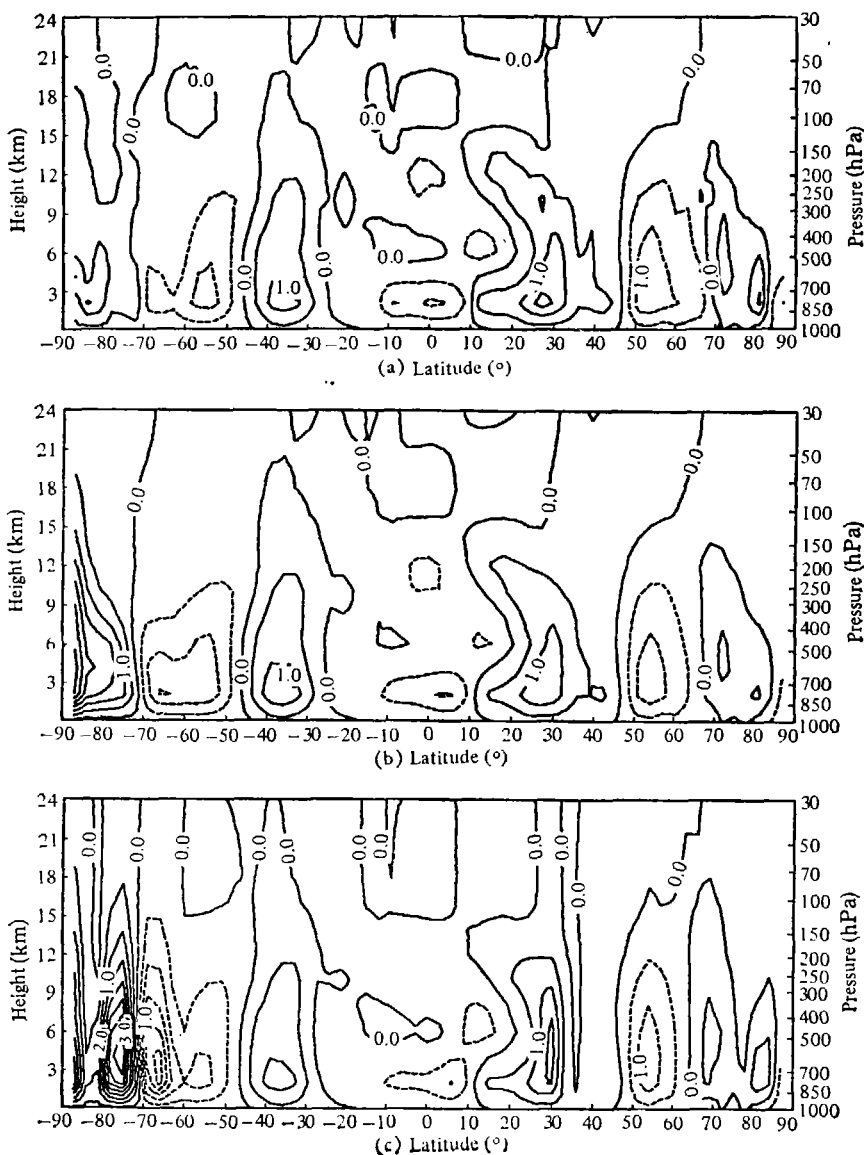


Fig. 7. The mean vertical wind  $\bar{\omega}$  of January 1982. Units in  $10^{-4}$  hPa  $\cdot$  s $^{-1}$ .  
 (a) Observations; (b) present scheme; (c) traditional scheme.



700 and 850 hPa and the higher near 200 hPa. On the contrary, there exist apparent errors in the  $\bar{\omega}$  test field of the traditional scheme: the upper rising centre becomes unclear; sinking near subtropics is in distortion; and even more serious errors appear at high latitudes.

It is worthwhile to point out that, if the data are not retrieved four times per day, then the traditional method gives even more severe distortions. For example, if only the data at 00Z and 12Z are included in the above calculations, the increase of the strength of the northern upper Hadley cell reaches about 50%, and the  $\bar{\omega}$  test field derived processes stronger distortions both in intensity and phase. This may be due to the semi-diurnal variations of the pressure fields.

## 2. Mean Meridional Circulation

From Fig. 6(a) and Table 1, we see that there are three cells in each hemisphere, with the stronger cells appearing in the winter hemisphere. The intensities of the southern and northern Hadley cells are  $27 \times 10^6 \text{ ton} \cdot \text{s}^{-1}$  and  $86 \times 10^6 \text{ ton} \cdot \text{s}^{-1}$  respectively. Compared to those of  $170 \times 10^6 \text{ ton} \cdot \text{s}^{-1}$  of Kidson et al.<sup>[9]</sup>, and of  $230 \times 10^6 \text{ ton} \cdot \text{s}^{-1}$  of Palmen and Vuorela<sup>[6]</sup>, but also of  $85 \times 10^6 \text{ ton} \cdot \text{s}^{-1}$  of Mintz and Lang<sup>[7]</sup> for the Hadley cell in the northern winter, our value seems too small. However, the strongest return flow of this Hadley cell at  $6^\circ\text{N}$  near 150 hPa in January 1982 is only  $1.58 \text{ m} \cdot \text{s}^{-1}$ , about half of its climatic mean (see Table A9 in Ref. [8]). The smallness of this Hadley cell may be reasonable and can be regarded as the results of the interannual variations of the mean meridional circulations.

As obtained by Wu and Liu<sup>[9]</sup> from the ECMWF analyses, instead of one simple centre in the tropical regions, the winter Hadley cell is composed of two centres. Our calculations also show that in addition to the lower tropospheric one of  $86 \times 10^6 \text{ ton} \cdot \text{s}^{-1}$ , there is an upper tropospheric centre of  $45 \times 10^6 \text{ ton} \cdot \text{s}^{-1}$ . Hollingsworth and Cats<sup>[10]</sup> pointed out that there can be two meridional return flows in the vertical in tropics if five normal modes are used in initialization, but only one if two modes are used merely. Numerical modelling of Schneider and Lindzen<sup>[11]</sup> showed that cumulus friction and detrainment in the upper troposphere can excite the upper cell, whereas surface temperature gradient is responsible for the lower cell. Recent experiments by Tiedtke (private communications) show that the centre of the July Southern Hemispheric Hadley cell can be lifted to much higher levels provided that shallow convection is parameterized in the model. All these suggest that the existence of double Hadley cell is possibly due to the thermal effects of sensible heating and shallow convection in the lower troposphere, and deep moist convection along the ITCZ.

## IV. DISCUSSIONS

At a latitude where there are mountains, the data under the ground surface must be extrapolated from the data above the surface. These fictitious "underground" data can result in considerable errors in the evolution of the zonal mean quantities, such as  $\bar{u}$ ,  $\bar{v}$ , and  $\bar{\omega}$ . Therefore, all methods of calculating the zonal mean merid-

ional circulations, including the present one, suffer from this data extrapolations. On the other hand, the upper layer observations are relatively reliable, especially over data dense areas. Our proposal is to keep these data as unchanged as possible in calculating the mean meridional circulation. The scheme of Section II was therefore developed along this line.

The discovery of the double cell structure of the Hadley cell has posed a new challenge to meteorologists concerning the dynamics and thermodynamics of tropical atmospheric motions. In any case, it is evident that further understanding of the nature and dynamics of the mean meridional circulations depends not only on more accurate data becoming more available, but also on the methodology used in processing the data.

We would like to thank Drs. A. Hollingsworth and A. Simmons for discussions during this work.

ECMWF offered all facilities for the study. The first author is indebted to his colleagues at ECMWF for their kind help.

#### REFERENCES

- [1] Lorenz, E. N., The nature and theory of the general circulation of the atmosphere, *WMO*, Geneva, 1967.
- [2] Eady, E. T., The cause of the general circulation of atmosphere, *Roy. Meteor. Soc. Cent. Proc.*, 1950, 156—172.
- [3] Green, J. S. A., Transfer properties of the large-scale eddies and the general circulation of the atmosphere, *Quart. J. Roy. Meteor. Soc.*, **96**(1970), 157—185.
- [4] Wu, Guoxiong & Tibaldi, S., Roles of mean meridional circulation in the atmosphere, *Scientia Atmospherica Sinica*, **12**(1988), 8—17.
- [5] Kidson, J. W., Vincent, D. G. & Newwell, R. E., Observational studies of the general circulation of the Tropics: long term mean values, *Quart. J. Roy. Meteor. Soc.*, **95**(1969), 258—287.
- [6] Palmen, E. & Vuorela, L., On the mean meridional circulations in the Northern Hemisphere during the winter season, *ibid.*, **89**(1963), 131—138.
- [7] Mintz, Y. & Lang, J., A model of the mean meridional circulation, Final Rept., Artical VI, Contract AF19 (122) 48, *Gen. Circ. Proj.*, U. C. L. A. 1955, 10.
- [8] Oort, A. H. & Rasmusson, E. M., Atmospheric circulation statistics, *NOAA*, professional paper 5, 1971.
- [9] 吴国雄、刘还珠, 时间平均全球大气环流统计, 气象出版社, 1987.
- [10] Hollingsworth, A. & Cats, G., Initialization in the tropics, *ECMWF Workshop on Tropical Meteorology and Its Effects on Medium Range Weather Prediction at Middle Latitudes*, ECMWF, Reading, England, 1981, 105—142.
- [11] Schneider, E. K. & Lindzen, R. S., Axially symmetric steady-state models of the basic state for instability and climatic studies, Part I: Linearized calculations, *J. Atmos. Sci.*, **34**(1977), 263—279.